Victor Iliev Rizov

DELAMINATION IN NONLINEAR ELASTIC MULTILAYERED BEAMS OF TRIPLE GRADED MATERIALS

DELAMINACIJA NELINEARNO ELASTIČNIH VIŠESLOJNIH NOSAČA OD TROSTRUKO GRADIJENTNIH MATERIJALA

Originalni naučni rad / Original scientific paper
UDK /UDC: 624.016.072.21.04

Rad primljen / Paper received: 11.09.2018

Adresa autora / Author's address:
University of Architecture, Civil Engineering and Geodesy, Depart. of Technical Mechanics, Sofia, Bulgaria,
email: v_rizov_fhe@uacg.bg

Keywords
- multilayered beam
- nonlinear elastic material
- delamination crack
- functionally graded material
- strain energy

Abstract

Delamination in nonlinear elastic multilayered double cantilever beam configurations of triple functionally graded materials is studied. The beam under consideration has an arbitrary number of longitudinal layers. Each layer has individual thickness and material properties. Besides, the material in each layer is functionally graded along the thickness, width and length of layer. A delamination crack is located arbitrary along the height of beam cross-section. Thus, the crack arms have different thicknesses. The beam is loaded by two bending moments of different magnitudes applied at the free ends of crack arms. The nonlinear fracture behaviour is studied in terms of the strain energy release rate. The solution derived is verified by analyzing the delamination crack with the help of the J-integral method. The solutions obtained are applied to investigate the influences of various geometrical and material parameters on the nonlinear delamination fracture in the considered multi-layered triple functionally graded beam configuration.

Ključne reči
- višeslojni nosač
- nelinearno elastičan materijal
- prslina delaminacije
- funkcionalni gradijentni materijal
- deformaciona energija

Izvod

Istražena je delaminacija kod konfiguracija tipa nelinearno elastičnog višeslojnog dvostruko usmerenog konzolnog nosača od trostruko gradijentnog materijala. Razmatrani nosač ima proizvoljan broj longitudinalnih slojeva. Svaki sloj datu debljinu i osobine materijala. Pored toga, u svakom sloju je materijal funkcionalan gradijentan u pravcima debljine, širine i dužine sloja. Prslina delaminacije je proizvoljno locirana u pravcu visine poprečnog preseka nosača. Stoga su raslojeni delovi prsline različite debljine. Nosač je opterećen sa dva momenta savijanja različitog intenziteta na slobodnim krajevima raslojenih ligamenata prsline. Nelinearni lom je proučen s obzirom na brzinu oslobađanja deformacione energije. Dobijeno rešenje je provereno analiziranjem prsline delaminacije primenom metode J integrala. Dobijena rešenja se koriste za istraživanje uticaja parametara geometrije i materijala na lom delaminacijom u konfiguracijama tipa višeslojnih trostruko gradijentnih nosača.

INTRODUCTION

Functionally graded materials play a vital role in the development of technologies in aerospace, microelectronics, engineering, optics and biomedicine, /1-6/. Basically, this is due to the fact that functionally graded materials permit tailoring of their microstructure and composition of their constituent materials in one or more spatial coordinates during manufacture (in this way, one can get optimum performance of structural members to external loads and influences, especially when the requirements of material properties are different in different parts of a member). Since macroscopic material properties of functionally graded materials vary smoothly, interfacial stress concentrations are eliminated which is one of the most important advantages of functionally graded materials over the laminated composites. Nevertheless, fracture is the earliest failure mode in structural members and components made of functionally graded materials.

Multilayered materials are an interesting class of inhomogeneous materials with numerous applications in engineering, electronics, aerospace and civil engineering. Multilayered materials are characterized by high strength to weight and stiffness to weight ratios in contrast to the traditional metal structural materials. Delamination fracture, i.e. separation of layers is crucial for structural integrity and durability of members and components made of multilayered materials. The importance of delemination fracture behaviour is confirmed by numerous investigations of various layered beam structures which are carried out by applying methods of linear elastic fracture mechanics assuming linear elastic behaviour of multilayered materials, /7/. Delamination fracture analyses of multilayered functionally graded beam configurations which exhibit nonlinear mechanical behaviour of the material are also performed, /8-12/. These analyses deal with multilayered beams made of materials which are functionally graded along the thickness or along the thickness and width of layers, /8-12/.

In this paper, analyses of a delamination crack in multilayered double cantilever beams made of materials which are functionally graded along the width, thickness and length of layers are developed. The nonlinear mechanical behaviour of the material is also taken into account in the delamination fracture analyses. Fracture is studied in terms of the strain energy release rate assuming that the coefficient in the power-law stress-strain relation is distributed continuously along the width, thickness and length of layers. The solution derived is verified by performing a delamination fracture analysis by applying the J-integral method. Parametric investigations of delamination fracture behaviour of the nonlinear elastic multilayered triple functionally graded beam configuration are carried out by using the solutions derived. For this purpose, effects of various geometrical and material parameters on the strain energy release rate and the J-integral are evaluated and discussed.

THEORERTICAL MODEL

The functionally graded multilayered double cantilever beam configuration analysed in the present paper is shown schematically in Fig. 1. The beam is made of an arbitrary number of horizontal layers. There is a delamination crack of length, a, located arbitrary along the beam height. The thicknesses of lower and upper crack arms are h_1 and h_2, respectively. Perfect adhesion is assumed between layers. Besides, each layer has individual thickness and material properties.

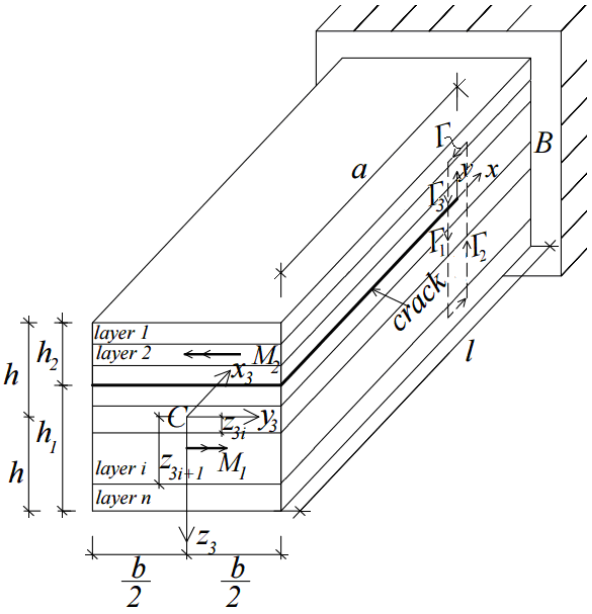

Figure 1. Schematic of the functionally graded multilayered double cantilever beam configuration.

The beam is loaded by two external moments, M_1 and M_2, applied on the free ends of lower and upper crack arms, respectively. The beam is clamped in section B. The cross-section of beam is a rectangle of width, b, and height, $2h$. The mechanical behaviour of the material is described by the following power-law stress-strain relation:

$$\sigma_i = D_i \varepsilon^{m_i}, \quad i = 1, 2, \ldots, n, \tag{1}$$

where: ε is the distribution of longitudinal strains; σ_i is the distribution of longitudinal normal stresses in the i-th layer; D_i and m_i are material properties in the same layer; n is the number of layers.

In each layer, the material is functionally graded along the width, thickness and length of the layer. In the cross-section of the i-th layer, the distribution of D_i is described by the following equation:

$$D_i = D_0 + \frac{16 y_3^4}{b^4} D_{K_i} + \frac{z_3^2}{h^2} D_{L_i}, \quad i = 1, 2, \ldots, n, \tag{2}$$

where: D_0 is the value of D_i in the centre of the beam cross-section; D_{Ki} and D_{Li} are material properties which govern the material gradient along the width and thickness of the layer, respectively.

The centroidal axes, y_3 and z_3, are shown in Fig. 1. The distribution of D_0 along the length of the beam is written as

$$D_0 = D_Q + \frac{x_3^4}{l^4} D_T, \tag{3}$$

where: D_Q is the value of D_0 in the free end of the beam; D_T is a material property which governs the material gradient along the beam length; x_3-axis is defined in Fig. 1. One can summarize that Eqs.(2) and (3) describe the distribution of D_0 in the multilayered beam under consideration.

The delamination fracture behaviour is analysed in terms of the strain energy release rate by applying the following formula, /8/:

$$G = \frac{dU^*}{bda}, \tag{4}$$

where: da is an elementary increase of the delamination crack length; dU^* is the change of complementary strain energy.

The beam complementary strain energy is written as

$$\begin{aligned} U^* = & \sum_{i=1}^{i=n_d} \int_{z_{1i}}^{z_{1i+1}} \left(\int_{-\frac{b}{2}}^{\frac{b}{2}} \int_0^a u^*_{0d_i} dx_1 dy_1 \right) dz_1 + \\ & + \sum_{i=1}^{i=n_g} \int_{z_{2i}}^{z_{2i+1}} \left(\int_{-\frac{b}{2}}^{\frac{b}{2}} \int_0^a u^*_{0g_i} dx_2 dy_2 \right) dz_2 + \\ & + \sum_{1=i}^{i=n} \int_{z_{4i}}^{z_{4i+1}} \left(\int_{-\frac{b}{2}}^{\frac{b}{2}} \int_a^l u^*_{0r_i} dx_4 dy_4 \right) dz_4 \end{aligned} \tag{5}$$

where: u^*_{0di}, u^*_{0gi} and u^*_{0ri} are the complementary strain energy densities in the i-th layer of the lower crack arm, upper crack arm, and un-cracked beam portion ($a \le x_3 \le l$), respectively.

Axes, x_1, y_1 and z_1, are shown in Fig. 2, x_2, y_2 and z_2 are the centroidal axes of the cross-section of upper crack arm (z_2 is directed downwards), x_4, y_4 and z_4 are the centroidal axes of the cross-section of un-cracked beam portion (z_4 is directed downwards), n_d and n_g are the numbers of layers in the lower and the upper crack arms, respectively.

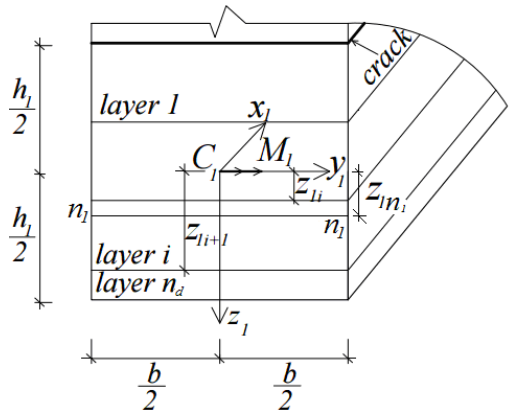

Figure 2. Geometry and loading of the free end of the lower crack arm ($n_1 - n_1$ is the neutral axis).

The complementary strain energy density in the i-th layer of lower crack arm is expressed as, /10/,

$$u_{0d_i}^{*} = D_i \frac{m_i \varepsilon^{m_i+1}}{m_i+1}. \tag{6}$$

The distribution of strains is analysed by applying the Bernoulli's hypothesis for plane sections since the span to height ratio of the considered beam is large. Concerning the application of Bernoulli's hypothesis in the present paper, it should also be mentioned that since the beam is loaded in pure bending (Fig. 1), the only non-zero strain is the longitudinal strain, ε. Therefore, according to the small strain compatibility equations, ε is distributed linearly along the height of the beam cross-section. Thus, ε in the lower crack arm is written as

$$\varepsilon = (z_1 - z_{1n_1})\kappa_1, \tag{7}$$

where: z_{1n1} is the coordinate of the neutral axis; κ_1 is the curvature of the lower crack arm. It should be noted that the neutral axis, $n_1 - n_1$, shifts from the centroid since the beam is multilayered and functionally graded, Fig. 2.

Quantities z_{1n1} and κ_1, in an arbitrary cross-section of the lower crack arm are determined from the following equilibrium equations:

$$N_1 = \sum_{i=1}^{i=n_d} \int_{z_{1i}}^{z_{1i+1}} \left(\int_{-\frac{b}{2}}^{\frac{b}{2}} \sigma dy_1 \right) dz_1, \tag{8}$$

$$M_{y_1} = \sum_{i=1}^{i=n_d} \int_{z_{1i}}^{z_{1i+1}} \left(\int_{-\frac{b}{2}}^{\frac{b}{2}} \sigma z_1 dy_1 \right) dz_1, \tag{9}$$

where: N_1 and M_{y1} are the axial force and bending moment, respectively. The coordinates z_{1i} and z_{1i+1}, are shown in Fig. 2. Obviously,

$$N_1 = 0, \quad M_{y1} = M_1. \tag{10}$$

In order to express the distribution of material property, D_i, in the cross-section of the i-th layer of the lower crack arm, Eq.(2) is re-written as

$$D_i = D_0 + \frac{16 y_3^4}{b^4} D_{K_i} + \frac{(\beta_d + z_1)^2}{h^2} D_{L_i}, \tag{11}$$

where: $\beta_d = h - h_1/2$. Then by substituting Eqs.(1), (2) and (7) in Eqs.(8) and (9), one derives

$$N_1 = \sum_{i=1}^{i=n_d} \left[\frac{D_0 b \kappa_1^{m_i}}{m_i+1} + \frac{D_{K_i} b \kappa_1^{m_i}}{5(m_i+1)} + \frac{D_{L_i} b \beta_d^2 \kappa_1^{m_i}}{h^2 (m_i+1)} \right] (\delta_i^{m_i+1} - \lambda_i^{m_i+1}) + \frac{2 D_{L_i} b \beta_d \kappa_1^{m_i}}{h^2} \left[\frac{1}{m_i+2} (\delta_i^{m_i+2} - \lambda_i^{m_i+2}) + \frac{z_{1n_1}}{m_i+1} (\delta_i^{m_i+1} - \lambda_i^{m_i+1}) \right] +$$
$$+ \frac{D_{L_i} b \kappa_1^{m_i} q_i}{h^2} \left[\frac{1}{f_i+3q_i} \left(\delta_i^{\frac{f_i+3q_i}{q_i}} - \lambda_i^{\frac{f_i+3q_i}{q_i}} \right) + \frac{2 z_{1n_1}}{f_i+2q_i} \left(\delta_i^{\frac{f_i+2q_i}{q_i}} - \lambda_i^{\frac{f_i+2q_i}{q_i}} \right) + \frac{z_{1n_1}^2}{f_i+q_i} \left(\delta_i^{\frac{f_i+q_i}{q_i}} - \lambda_i^{\frac{f_i+q_i}{q_i}} \right) \right], \tag{12}$$

$$M_{y_1} = \sum_{i=1}^{i=n_d} \left(D_0 b \kappa_1^{m_i} + \frac{D_{K_i} b \kappa_1^{m_i}}{5} + \frac{D_{L_i} b \beta_d^2 \kappa_1^{m_i}}{h^2} \right) \left[\frac{1}{m_i+2} (\delta_i^{m_i+2} - \lambda_i^{m_i+2}) + \frac{z_{1n_1}}{m_i+1} (\delta_i^{m_i+1} - \lambda_i^{m_i+1}) \right] + \frac{2 D_{L_i} b \beta_d \kappa_1^{m_i} q_i}{h^2} \times$$
$$\times \left[\frac{1}{f_i+3q_i} \left(\delta_i^{\frac{f_i+3q_i}{q_i}} - \lambda_i^{\frac{f_i+3q_i}{q_i}} \right) + + \frac{2 z_{1n_1}}{f_i+2q_i} \left(\delta_i^{\frac{f_i+2q_i}{q_i}} - \lambda_i^{\frac{f_i+2q_i}{q_i}} \right) + \frac{z_{1n_1}^2}{f_i+q_i} \left(\delta_i^{\frac{f_i+q_i}{q_i}} - \lambda_i^{\frac{f_i+q_i}{q_i}} \right) \right] + \frac{D_{L_i} b \kappa_1^{m_i} q_i}{h^2} \times \tag{13}$$
$$\times \left[\frac{1}{f_i+4q_i} \left(\delta_i^{\frac{f_i+4q_i}{q_i}} - \lambda_i^{\frac{f_i+4q_i}{q_i}} \right) + \frac{3 z_{1n_1}}{f_i+3q_i} \left(\delta_i^{\frac{f_i+3q_i}{q_i}} - \lambda_i^{\frac{f_i+3q_i}{q_i}} \right) + \frac{3 z_{1n_1}^2}{f_i+2q_i} \left(\delta_i^{\frac{f_i+2q_i}{q_i}} - \lambda_i^{\frac{f_i+2q_i}{q_i}} \right) + \frac{z_{1n_1}^3}{f_i+q_i} \left(\delta_i^{\frac{f_i+q_i}{q_i}} - \lambda_i^{\frac{f_i+q_i}{q_i}} \right) \right],$$

where: $\delta_i = z_{1i+1} - z_{1n1}$, $\lambda_i = z_{1i} - z_{1n1}$, and $f_i/q_i = m_i$ (f_i and q_i are positive integers).

Equations (12) and (13) should be solved with respect to z_{1n1} and κ_1 by applying the MatLab computer program. It should be mentioned that Eqs.(12) and (13) can be used to determine z_{1n1} and κ_1 in any cross-section of the lower crack arm. The only difference in various cross-sections is the value of D_0 that is determined by Eq.(3).

By substituting D_i and ε in Eq.(6), the distribution of complementary strain energy density in the i-th layer of the lower crack arm is re-written as

$$u_{0d}^{*} = \left[D_0 + \frac{16 y_1^4}{b^4} D_{K_i} + \frac{(\beta_d + z_1)^2}{h^2} D_{L_i} \right] \frac{m_i (z_1 - z_{1n_1})^{m_i+1} \kappa_1^{m_i+1}}{m_i+1} \tag{14}$$

Equation (14) can also be used to calculate the distribution of complementary strain energy density, u^{*}_{0gi}, in the i-th

layer of the upper crack arm. For this purpose, y_1, z_1, β_d, z_{1n1} and κ_1 have to be replaced respectively with y_2, z_2, β_g, z_{2n2} and κ_2, where $\beta_g = -h + h_1/2$, z_{2n2} and κ_2 are the neutral axis coordinate and the curvature of the upper crack arm. The quantities, z_{2n2} and κ_2, can be obtained from equilibrium Eqs.(12) and (13). For this purpose, n_d, M_{y1}, z_{1i}, z_{1i+1}, β_d, z_{1n1} and κ_1 have to be replaced with n_g, M_2, z_{2i}, z_{2i+1}, β_g, z_{2n2} and κ_2, respectively.

Equation (14) can also be applied to calculate the distribution of complementary strain energy density, u^*_{0ri}, in the i-th layer of the un-cracked beam portion. For this purpose, y_1, z_1, β_d, z_{1n1} and κ_1 have to be replaced with y_4, z_4, 0, z_{4n4} and κ_4, respectively (z_{4n4} and κ_4 are the neutral axis coordinate and the curvature of the un-cracked beam portion, in respect). Equations (12) and (13) can be used to determine z_{4n4} and κ_4. For this purpose, n_d, M_{y1}, z_{1i}, z_{1i+1}, β_d, z_{1n1} and κ_1 have to be replaced with n, $M_1 - M_2$, z_{4i}, z_{4i+1}, 0, z_{4n4} and κ_4, respectively.

By substituting u^*_{0di}, u^*_{0gi}, u^*_{0ri} and Eq.(5) in Eq. (4), one derives the following formula for the calculation of strain energy release rate in the functionally graded multilayered double cantilever beam:

$$G=\sum_{i=1}^{i=n_d}\frac{m_i\kappa_1^{m_i+1}}{b(m_i+1)}\left\{\left[\frac{D_0 b}{m_{u_i}+1}+\frac{D_{K_i}b}{5\left(m_{u_i}+1\right)}+\frac{D_{L_i}b\beta_d^2}{h^2\left(m_{u_i}+1\right)}\right]\left(\delta_i^{m_{u_i}+1}-\lambda_i^{m_{u_i}+1}\right)+\frac{2D_{L_i}b\beta_d}{h^2}\left[\frac{1}{m_{u_i}+2}(\delta_i^{m_{u_i}+2}-\lambda_i^{m_{u_i}+2})+\frac{z_{1n_1}}{m_{u_i}+1}(\delta_i^{m_{u_i}+1}-\lambda_i^{m_{u_i}+1})\right]+\right.$$
$$\left.+\frac{D_{L_i}bq_{u_i}}{h^2}\left[\frac{1}{f_{u_i}+3q_{u_i}}\left(\delta_i^{\frac{f_{u_i}+3q_{u_i}}{q_{u_i}}}-\lambda_i^{\frac{f_{u_i}+3q_{u_i}}{q_{u_i}}}\right)+\frac{2z_{1n_1}}{f_{u_i}+2q_{u_i}}\left(\delta_i^{\frac{f_{u_i}+2q_{u_i}}{q_{u_i}}}-\lambda_i^{\frac{f_{u_i}+2q_{u_i}}{q_{u_i}}}\right)+\frac{z_{1n_1}^2}{f_{u_i}+q_{u_i}}\left(\delta_i^{\frac{f_{u_i}+q_{u_i}}{q_i}}-\lambda_i^{\frac{f_{u_i}+q_{u_i}}{q_{u_i}}}\right)\right]\right\}+$$
$$+\sum_{i=1}^{i=n_g}\frac{m_i\kappa_2^{m_i+1}}{b(m_i+1)}\left\{\left[\frac{D_0 b}{m_{u_i}+1}+\frac{D_{K_i}b}{5(m_{u_i}+1)}+\frac{D_{L_i}b\beta_g^2}{h^2(m_{u_i}+1)}\right](\delta_{gi}^{m_{u_i}+1}-\lambda_{gi}^{m_{u_i}+1})+\frac{2D_{L_i}b\beta_g}{h^2}\left[\frac{1}{m_{u_i}+2}(\delta_{gi}^{m_{u_i}+2}-\lambda_{gi}^{m_{u_i}+2})+\frac{z_{2n_2}}{m_{u_i}+1}(\delta_{gi}^{m_{u_i}+1}-\lambda_{gi}^{m_{u_i}+1})\right]+\right.$$
$$\left.+\frac{D_{L_i}bq_{u_i}}{h^2}\left[\frac{1}{f_{u_i}+3q_{u_i}}\left(\delta_{gi}^{\frac{f_{u_i}+3q_{u_i}}{q_{u_i}}}-\lambda_{gi}^{\frac{f_{u_i}+3q_{u_i}}{q_{u_i}}}\right)\right.\right.\left.\left.+\frac{2z_{2n_2}}{f_{u_i}+2q_{u_i}}\left(\delta_{gi}^{\frac{f_{u_i}+2q_{u_i}}{q_{u_i}}}-\lambda_{gi}^{\frac{f_{u_i}+2q_{u_i}}{q_{u_i}}}\right)+\frac{z_{2n_2}^2}{f_{u_i}+q_{u_i}}\left(\delta_{gi}^{\frac{f_{u_i}+q_{u_i}}{q_i}}-\lambda_{gi}^{\frac{f_{u_i}+q_{u_i}}{q_{u_i}}}\right)\right]\right\}-$$
$$-\sum_{i=1}^{i=n}\frac{m_i\kappa_4^{m_i+1}}{b(m_i+1)}\left\{\left[\frac{D_0 b}{m_{u_i}+1}+\frac{D_{K_i}b}{5(m_{u_i}+1)}\right](\delta_{ri}^{m_{u_i}+1}-\lambda_{ri}^{m_{u_i}+1})+\frac{D_{L_i}bq_{u_i}}{h^2}\left[\frac{1}{f_{u_i}+3q_{u_i}}\left(\delta_{ri}^{\frac{f_{u_i}+3q_{u_i}}{q_{u_i}}}-\lambda_{ri}^{\frac{f_{u_i}+3q_{u_i}}{q_{u_i}}}\right)+\frac{2z_{4n_4}}{f_{u_i}+2q_{u_i}}\left(\delta_{ri}^{\frac{f_{u_i}+2q_{u_i}}{q_{u_i}}}-\lambda_{ri}^{\frac{f_{u_i}+2q_{u_i}}{q_{u_i}}}\right)+\right.\right.$$
$$\left.\left.+\frac{z_{4n_4}^2}{f_{u_i}+q_{u_i}}\left(\delta_{ri}^{\frac{f_{u_i}+q_{u_i}}{q_i}}-\lambda_{ri}^{\frac{f_{u_i}+q_{u_i}}{q_{u_i}}}\right)\right]\right\} \qquad (15)$$

where: $m_{ui} = m_i + 1$, $f_{ui}/q_{ui} = m_{ui}$ (f_{ui} and q_{ui} are positive integers), $\delta_{gi} = z_{2i+1} - z_{2n2}$, $\lambda_{gi} = z_{2i} - z_{2n2}$, $\delta_{ri} = z_{4i+1} - z_{4n4}$ and $\lambda_{ri} = z_{4i} - z_{4n4}$. In Eq.(15), D_0, z_{1n1}, κ_1, z_{2n2}, κ_2, z_{4n4} and κ_4 are obtained by Eqs.(3), (12) and (13) at $x_3 = a$. Thus, Eq.(15) can be applied to calculate the strain energy release rate at any crack length in the interval, $0 \le a \le l$.

The delamination fracture is analysed also by applying the J-integral approach, /13/, in order to verify Eq.(15). The J-integral is solved by using the integration contour, Γ, shown by dashed line in Fig. 1. It is obvious that the J-integral value is non-zero only in segments, Γ_1, Γ_2 and Γ_3, of the integration contour (Γ_1, Γ_2 and Γ_3 coincide with the free end of the lower crack arm, the clamping and the free end of the upper crack arm, respectively). Therefore, the J-integral solution is written as

$$J = J_{\Gamma_1} + J_{\Gamma_2} + J_{\Gamma_3}, \qquad (16)$$

where: $J_{\Gamma 1}$, $J_{\Gamma 2}$ and $J_{\Gamma 3}$ are the J-integral values in segments Γ_1, Γ_2 and Γ_3, respectively.

The J-integral in segment Γ_1, is written as

$$J_{\Gamma_1}=\sum_{i=1}^{n_d}\int_{z_{1i}}^{z_{1i+1}}\left[u_{0d_i}\cos\alpha-\left(p_{xi}\frac{\partial u}{\partial x}+p_{yi}\frac{\partial v}{\partial x}\right)\right]ds, \qquad (17)$$

where: α is the angle between the outwards normal vector to the contour of integration and crack direction; p_{xi} and p_{yi} are the components of stress vector in the i-th layer of the lower crack arm; u and v are the components of displacement vector with respect to the crack tip coordinate system xy (x is directed along the crack); ds is a differential element along the contour.

The J-integral components in segment Γ_1 of the integration contour are written as

$$p_{xi} = -\sigma_i = -D_i\varepsilon^{m_i}, \quad p_{yi} = 0, \qquad (18)$$

$$ds = dz_1, \quad \cos\alpha = -1, \qquad (19)$$

where: coordinate z_1 varies in the interval $[-h_1/2, h_1/2]$.

The strain energy density in the i-th layer of the lower crack arm is obtained as, /10/,

$$u_{0d_i} = \frac{D_i \varepsilon^{m_i+1}}{m_i+1}. \tag{20}$$

The partial derivative $\partial u/\partial x$ that participates in Eq.(17) is written as

$$\frac{\partial u}{\partial x} = \varepsilon = (z_1 - z_{1n_1})\kappa_1. \tag{21}$$

By combining Eqs.(1), (17), (18), (19), (20) and (21), the solution of $J_{\Gamma 1}$ is derived as

$$J_{\Gamma_1} = \sum_{i=1}^{i=n_d} \frac{m_i \kappa_1^{m_i+1}}{b(m_i+1)} \left\{ \left[\frac{D_0 y_1}{m_{u_i}+1} + \frac{16 D_{K_i} y_1^4}{b^4 (m_{u_i}+1)} + \frac{D_{L_i} \beta_d^2 y_1}{h^2 (m_{u_i}+1)} \right] \left(\delta_i^{m_{u_i}+1} - \lambda_i^{m_{u_i}+1} \right) + \frac{2 D_{L_i} y_1 \beta_d}{h^2} \left[\frac{1}{m_{u_i}+2} (\delta_i^{m_{u_i}+2} - \lambda_i^{m_{u_i}+2}) + \frac{z_{1n_1}}{m_{u_i}+1} (\delta_i^{m_{u_i}+1} - \lambda_i^{m_{u_i}+1}) \right] + \right.$$
$$\left. + \frac{D_{L_i} y_1 q_{u_i}}{h^2} \left[\frac{1}{f_{u_i}+3q_{u_i}} \left(\delta_i^{\frac{f_{u_i}+3q_{u_i}}{q_{u_i}}} - \lambda_i^{\frac{f_{u_i}+3q_{u_i}}{q_{u_i}}} \right) + \frac{2 z_{1n_1}}{f_{u_i}+2q_{u_i}} \left(\delta_i^{\frac{f_{u_i}+2q_{u_i}}{q_{u_i}}} - \lambda_i^{\frac{f_{u_i}+2q_{u_i}}{q_{u_i}}} \right) + \frac{z_{1n_1}^2}{f_{u_i}+q_{u_i}} \left(\delta_i^{\frac{f_{u_i}+q_{u_i}}{q_i}} - \lambda_i^{\frac{f_{u_i}+q_{u_i}}{q_{u_i}}} \right) \right] \right\}, \tag{22}$$

where: z_{1n1} and κ_1 are determined from Eqs.(12) and (13). In Eq.(23) the coordinate y_1 varies in the interval $[-b/2, b/2]$.

Equation (22) can be applied also to obtain the solution of J-integral in segment Γ_2 of the integration contour (Fig. 1). For this purpose, n_d, z_{1i}, z_{1i+1}, β_d, δ_i, λ_i, z_{1n1} and κ_1 have to be replaced with n, z_{4i}, z_{4i+1}, 0, δ_{ri}, λ_{ri}, z_{4n4} and κ_4, in respect. Besides, the sign of Eq.(23) must be set to 'minus' since the contour of integration is directed upwards in segment Γ_2.

Also, Eq.(22) is applied to obtain the J-integral solution in segment Γ_3, of the integration contour (Fig. 1). For this purpose, n_d, z_{1i}, z_{1i+1}, β_d, δ_i, λ_i, z_{1n1} and κ_1 are replaced with n_g, z_{2i}, z_{2i+1}, β_g, δ_{gi}, λ_{gi}, z_{2n2} and κ_2, respectively.

The J-integral solution is derived by substituting $J_{\Gamma 1}$, $J_{\Gamma 2}$ and $J_{\Gamma 3}$ in Eq.(17):

$$J = \sum_{i=1}^{i=n_d} \frac{m_i \kappa_1^{m_i+1}}{b(m_i+1)} \left\{ \left[\frac{D_0 y_1}{m_{u_i}+1} + \frac{16 D_{K_i} y_1^4}{b^4 (m_{u_i}+1)} + \frac{D_{L_i} \beta_d^2 y_1}{h^2 (m_{u_i}+1)} \right] \left(\delta_i^{m_{u_i}+1} - \lambda_i^{m_{u_i}+1} \right) + \frac{2 D_{L_i} y_1 \beta_d}{h^2} \left[\frac{1}{m_{u_i}+2} \left(\delta_i^{m_{u_i}+2} - \lambda_i^{m_{u_i}+2} \right) + \frac{z_{1n_1}}{m_{u_i}+1} \left(\delta_i^{m_{u_i}+1} - \lambda_i^{m_{u_i}+1} \right) \right] + \right.$$
$$\left. + \frac{D_{L_i} y_1 q_{u_i}}{h^2} \left[\frac{1}{f_{u_i}+3q_{u_i}} \left(\delta_i^{\frac{f_{u_i}+3q_{u_i}}{q_{u_i}}} - \lambda_i^{\frac{f_{u_i}+3q_{u_i}}{q_{u_i}}} \right) + \frac{2 z_{1n_1}}{f_{u_i}+2q_{u_i}} \left(\delta_i^{\frac{f_{u_i}+2q_{u_i}}{q_{u_i}}} - \lambda_i^{\frac{f_{u_i}+2q_{u_i}}{q_{u_i}}} \right) + \frac{z_{1n_1}^2}{f_{u_i}+q_{u_i}} \left(\delta_i^{\frac{f_{u_i}+q_{u_i}}{q_i}} - \lambda_i^{\frac{f_{u_i}+q_{u_i}}{q_{u_i}}} \right) \right] \right\} +$$
$$+ \sum_{i=1}^{i=n_g} \frac{m_i \kappa_2^{m_i+1}}{b(m_i+1)} \left\{ \left[\frac{D_0 y_1}{m_{u_i}+1} + \frac{16 D_{K_i} y_1^4}{b^4 (m_{u_i}+1)} + \frac{D_{L_i} \beta_g^2 y_1}{h^2 (m_{u_i}+1)} \right] \left(\delta_{gi}^{m_{u_i}+1} - \lambda_{gi}^{m_{u_i}+1} \right) + \frac{2 D_{L_i} y_1 \beta_g}{h^2} \left[\frac{1}{m_{u_i}+2} \left(\delta_{gi}^{m_{u_i}+2} - \lambda_{gi}^{m_{u_i}+2} \right) + \frac{z_{2n_2}}{m_{u_i}+1} \left(\delta_{gi}^{m_{u_i}+1} - \lambda_{gi}^{m_{u_i}+1} \right) \right] + \right.$$
$$\left. + \frac{D_{L_i} y_1 q_{u_i}}{h^2} \left[\frac{1}{f_{u_i}+3q_{u_i}} \left(\delta_{gi}^{\frac{f_{u_i}+3q_{u_i}}{q_{u_i}}} - \lambda_{gi}^{\frac{f_{u_i}+3q_{u_i}}{q_{u_i}}} \right) + \frac{2 z_{2n_2}}{f_{u_i}+2q_{u_i}} \left(\delta_{gi}^{\frac{f_{u_i}+2q_{u_i}}{q_{u_i}}} - \lambda_{gi}^{\frac{f_{u_i}+2q_{u_i}}{q_{u_i}}} \right) + \frac{z_{2n_2}^2}{f_{u_i}+q_{u_i}} \left(\delta_{gi}^{\frac{f_{u_i}+q_{u_i}}{q_i}} - \lambda_{gi}^{\frac{f_{u_i}+q_{u_i}}{q_{u_i}}} \right) \right] \right\} -$$
$$- \sum_{i=1}^{i=n} \frac{m_i \kappa_4^{m_i+1}}{b(m_i+1)} \left\{ \left[\frac{D_0 y_1}{m_{u_i}+1} + \frac{16 D_{K_i} y_1^4}{b^4 (m_{u_i}+1)} \right] \left(\delta_{ri}^{m_{u_i}+1} - \lambda_{ri}^{m_{u_i}+1} \right) + \frac{D_{L_i} y_1 q_{u_i}}{h^2} \left[\frac{1}{f_{u_i}+3q_{u_i}} \left(\delta_{ri}^{\frac{f_{u_i}+3q_{u_i}}{q_{u_i}}} - \lambda_{ri}^{\frac{f_{u_i}+3q_{u_i}}{q_{u_i}}} \right) + \frac{2 z_{4n_4}}{f_{u_i}+2q_{u_i}} \left(\delta_{ri}^{\frac{f_{u_i}+2q_{u_i}}{q_{u_i}}} - \lambda_{ri}^{\frac{f_{u_i}+2q_{u_i}}{q_{u_i}}} \right) + \right. \right.$$
$$\left. \left. + \frac{z_{4n_4}^2}{f_{u_i}+q_{u_i}} \left(\delta_{ri}^{\frac{f_{u_i}+q_{u_i}}{q_i}} - \lambda_{ri}^{\frac{f_{u_i}+q_{u_i}}{q_{u_i}}} \right) \right] \right\}. \tag{23}$$

Equation (23) describes the distribution of J-integral value along the delamination crack front since $-b/2 \le y_1 \le b/2$. It should be mentioned that the parameters, D_0, z_{1n1}, κ_1, z_{2n2}, κ_2, z_{4n4} and κ_4, which are involved in Eq.(24) are determined by Eqs.(3), (12) and (13) at $x_3 = a$. Thus, one can use Eq.(23) to investigate the J-integral value distribution along the crack front at any crack length in the interval $0 < a < l$.

The average value of J-integral along the delamination crack front is written as

$$J_{AV} = \frac{1}{b} \int_{-\frac{b}{2}}^{\frac{b}{2}} J dy_1. \tag{24}$$

It should be mentioned that the J-integral obtained by substituting Eq.(23) in Eq.(24) matches exactly Eq.(15) for the strain energy release rate. This fact is a verification of the delamination fracture analysis of the nonlinear elastic multilayered triple functionally graded beam configuration developed in the present study.

NUMERICAL RESULTS AND DISCUSSION

The effects of crack location along the height of the beam cross-section, the material gradients along the width, thickness and length of layers, the nonlinear mechanical behaviour of the material and the crack length on the delamination fracture in the multilayered triple functionally graded beam are evaluated. For this purpose, calculations of the strain energy release rate are carried-out by applying Eq.(15). Two functionally graded beam configurations made of three longitudinal layers are considered in order to evaluate the influence of the crack location along the height of the beam cross-section (Fig. 3). The thickness of each layer is t_l. In the configuration shown in Fig. 3a the crack is located between layers 2 and 3. A delamination crack between layers 1 and 2 is also analysed (Fig. 3b). It is assumed that $b = 0.010$ m, $h = 0.0015$ m, $t_l = 0.001$ m, $M_1 = 15$ Nm and $M_2 = 20$ Nm. The strain energy release rate is presented in non-dimensional form by using the formula $G_N = G/(D_Q b)$. The material gradient along the width of layer 3 is characterized by D_{K3}/D_Q ratio. The position of the delamination crack front along the beam length is characterized by a/l ratio. It is assumed that $D_{K1}/D_Q = 0.6$, $D_{L1}/D_{K1} = 0.7$, $D_{K2}/D_Q = 0.7$, $D_{L2}/D_{K2} = 0.8$, $D_{L3}/D_{K3} = 2$, $D_T/D_Q = 0.5$, $a/l = 0.3$, $m_1 = m_2 = m_3 = 0.8$, $f_1 = f_2 = f_3 = 8$, $q_1 = q_2 = q_3 = 10$, $m_{u1} = m_{u2} = m_{u3} = 1.8$, $f_{u1} = f_{u2} = f_{u3} = 18$ and $q_{u1} = q_{u2} = q_{u3} = 10$. The strain energy release rate in non-dimensional form is plotted against D_{K3}/D_Q ratio in Fig. 4 for the two three-layered functionally graded beam configurations (refer to Fig. 3). The curves in Fig. 4 indicate that the strain energy release rate decreases with increasing of D_{K3}/D_Q ratio. This finding is attributed to the increase of the beam stiffness. Figure 4 shows also that the strain energy release rate increases when the crack location changes from this in Fig. 3a to that in Fig. 3b.

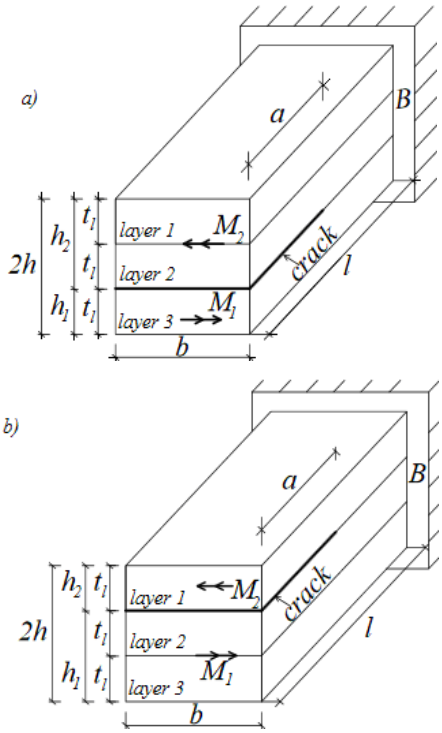

Figure 3. Two three-layered functionally graded double cantilever beam configurations with a delamination crack located between (*a*) layers 2 and 3 and (*b*) layers 1 and 2.

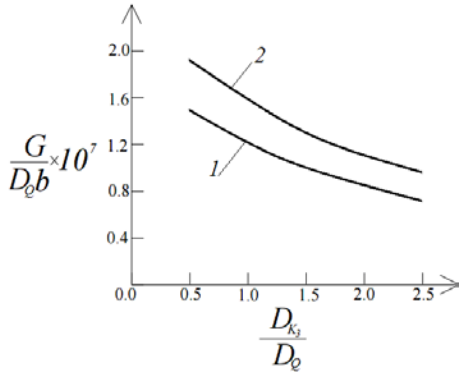

Figure 4. The strain energy release rate in non-dimensional form plotted against D_{K3}/D_Q ratio (curve 1 - for crack located between layers 2 and 3 and curve 2 - for crack between layers 1 and 2).

The influence of D_{L3}/D_Q ratio on the delamination fracture is also analysed. The beam configuration shown in Fig. 3a is considered. The strain energy release rate in non-dimensional form is plotted against D_{L3}/D_Q ratio at $D_{K3}/D_Q = 0.5$ in Fig. 5. It can be observed that the strain energy release rate decreases with increasing of D_{L3}/D_Q ratio (Fig. 5). The effect of nonlinear mechanical behaviour of material on the delamination fracture is evaluated too. For this purpose, the strain energy release rate derived assuming linear-elastic behaviour of the functionally graded material is shown in non-dimensional form as a function of D_{L3}/D_Q ratio in Fig. 5 for comparison with the nonlinear solution (the linear-elastic solution is obtained by substituting $m_1 = m_2 = m_3 = 1$ in Eq.(15)). The curves in Fig. 5 indicate that the material nonlinearity leads to increase of the strain energy release rate.

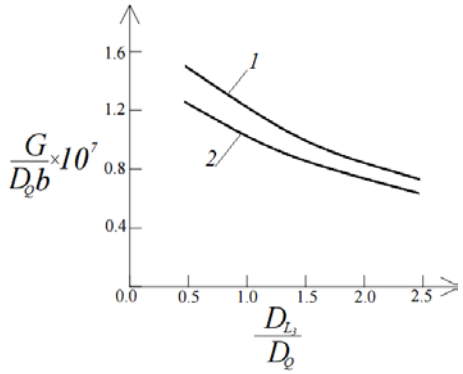

Figure 5. The strain energy release rate in non-dimensional form presented as a function of D_{L3}/D_Q ratio (curve 1 – at nonlinear elastic behaviour of the material, curve 2 – at linear-elastic behaviour of the material).

The effect of material gradient along the beam length on the nonlinear delamination fracture behaviour is analysed too. The beam configuration shown in Fig. 3a is investigated. The material gradient along the beam length is characterized by D_T/D_Q ratio.

The strain energy release rate in non-dimensional form is plotted against D_T/D_Q ratio in Fig. 6 at two a/l ratios. One can observe in Fig. 6 that the strain energy release rate

decreases with increasing of D_T/D_Q ratio (this behaviour is due to the increase of the beam stiffness). It can be observed also that the strain energy release rate decreases with increasing of a/l ratio (Fig. 6). This finding is explained with increase of the value of D_0 in the beam cross-section in which the delamination crack front is located.

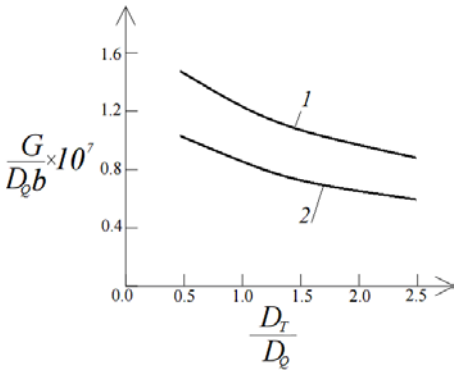

Figure 6. The strain energy release rate in non-dimensional form presented as a function of D_T/D_Q ratio (curve *1* – at $a/l = 0.3$, curve 2 – at $a/l = 0.6$).

The influence of material gradient on the distribution of the J-integral value along the delamination crack front is investigated. For this purpose, calculations are performed by using Eq.(23). Coordinate y_1, is varied in the interval $[-b/2, b/2]$. The J-integral value is presented in non-dimensional form by using the formula $J_N = J/(D_Q b)$. The beam configuration shown in Fig. 3a is considered. Two patterns of material gradient are analysed. Pattern 1 is characterized by $D_{K1}/D_Q = -0.4$, $D_{L1}/D_{K1} = 1.5$, $D_{K2}/D_Q = -0.4$, $D_{L2}/D_{K2} = 2$, $D_{K3}/D_Q = -0.4$ and $D_{L3}/D_{K3} = 1.2$. Pattern 2 of material gradient is characterized by $D_{K1}/D_Q = 1.3$, $D_{L1}/D_{K1} = 1.5$, $D_{K2}/D_Q = 1.3$, $D_{L2}/D_{K2} = 2$, $D_{K3}/D_Q = 1.3$ and $D_{L3}/D_{K3} = 1.2$. The distribution of the J-integral value in non-dimensional form along the delamination crack front at the two patterns of material gradient is presented in Fig. 7 at $a/l = 0.3$. Only the right-hand half of the delamination crack front is shown in Fig. 7 since the distribution is symmetrical with respect to the crack front centre. The horizontal axis is defined such that $2y_1/b = 0.0$ is in the delamination crack front centre. Thus, $2y_1/b = 1$ is in the right-hand lateral surface of the beam. It can be observed in Fig. 7 that for pattern 1 the J-integral value is minimal in the crack front centre and gradually increases towards the right-hand lateral surface of the beam. Thus finding is attributed to the fact that for pattern 1 the material property, D_i, gradually decreases towards the beam lateral surfaces. Figure 7 shows also that for pattern 2 the J-integral value decreases towards the right-hand lateral surface of the beam.

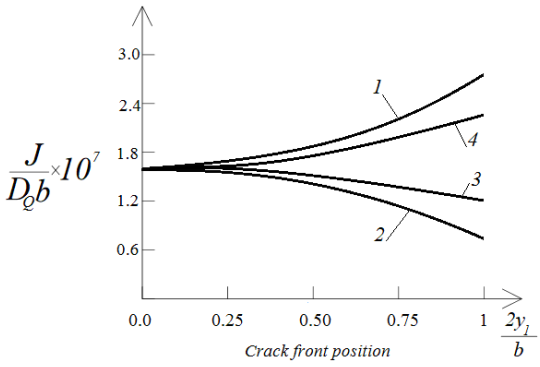

Figure 7. The distribution of the J-integral value in non-dimensional form along the delamination crack front (curve 1 - at pattern 1 of material gradient, curve 2 – at pattern 2 of material gradient, curve 3 – at pattern 3 of material gradient, curve 4 at pattern 4 of material gradient).

The distribution of the J-integral value along the delamination crack front is analysed also at pattern 3 and pattern 4 of material gradient.

Pattern 3 is characterized by $D_{K1}/D_Q = -0.2$, $D_{L1}/D_{K1} = 1.5$, $D_{K2}/D_Q = -0.2$, $D_{L2}/D_{K2} = 2$, $D_{K3}/D_Q = -0.2$ and $D_{L3}/D_{K3} = 1.2$, while pattern 4 is characterized by $D_{K1}/D_Q = 1.2$, $D_{L1}/D_{K1} = 1.5$, $D_{K2}/D_Q = 1.2$, $D_{L2}/D_{K2} = 2$, $D_{K3}/D_Q = 1.2$ and $D_{L3}/D_{K3} = 1.2$. The distribution of the J-integral value along the delamination crack front for patterns 3 and 4 is shown also in Fig. 7.

The effect of the delaminaton crack length on the J-integral value distribution along the crack front is also investigated. For this purpose, the J-integral value distribution along the crack front is shown in Fig. 8 at two a/l ratios for pattern 1 of material gradient. The curves in Fig. 8 indicate that the J-integral value decreases with increasing of the crack length. Besides, the J-integral value increases towards the beam lateral surface.

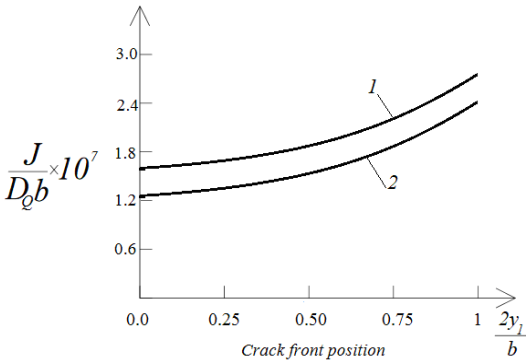

Figure 8. The distribution of the J-integral value in non-dimensional form along the delamination crack front (curve 1 – at $a/l = 0.3$, curve 2 – at $a/l = 0.6$).

CONCLUSIONS

Analyses of the delamination fracture in nonlinear elastic multilayered double cantilever beams made of materials which are functionally graded along the width, thickness and length of layers are developed. The fracture behaviour is studied in terms of the strain energy release rate. The solution derived is verified by analysing the fracture with the help of the J-integral. It should be noted that the solution to the J-integral obtained in the present paper can be used to investigate the distribution of the J-integral value along the crack front as a function of the crack length. The solution to the strain energy release rate is applicable for beams made of an arbitrary number of layers. Also, each layer has individual thickness and material properties. Besides, the material in each layer is triple functionally graded. The delamination crack is located arbitrary along the height of the beam cross-section. The solution derived is applied to evaluate the effects of crack location, material

gradients in width, thickness and length directions of layers, crack length and nonlinear mechanical behaviour of the material on the delamination fracture. The analysis reveals that the strain energy release rate decreases with increasing of D_{K3}/D_Q, D_{L3}/D_Q and D_T/D_Q ratios. This finding is attributed to the increase of the beam stiffness. The dependency of the distribution of the J-integral value along the delamination crack front on the material gradients is investigated too. It is found that the J-integral value is distributed non-uniformly along the delamination crack front (the distribution is strongly influenced by the material gradient along the beam width). The analysis shows also that the J-integral value decreases with increasing of the crack length. The nonlinear elastic solution for the strain energy release rate is compared with the linear-elastic one. It is found that the material nonlinearity leads to increase of the strain energy release rate. The effect of the crack length on the fracture behaviour is also investigated. It is found that the strain energy release rate decreases with increasing of the crack length (this is due to the increase of the value of D_0 in the beam cross-section in which the crack front is located).

REFERENCES

1. Suresh, S., Mortensen, A., Fundamentals of Functionally Graded Materials, IOM Communications Ltd, London, 1998.
2. Hirai, T., Chen, L. (1999), Recent and prospective development of functionally graded materials in Japan, Mater Sci. Forum, 308-311(2): 509-514.
3. Gasik, M. (2010), *Functionally graded materials: bulk processing techniques,* Int. J Mater. Prod. Tech. 39(1-2):20-29. doi: 10.1504/IJMPT.2010.034257
4. Hedia, H.S., et al. (2014), *A new design of cemented stem using functionally graded materials (FGM)*, Biomed. Mater. Eng. 24 (3): 1575-1588. doi: 10.3233/BME-140962
5. Yan, W., et al. (2016), *Multi-scale modelling of electron-beam melting of functionally graded materials*. Acta Mater. 115: 403 -412. doi: 10.1016/j.actamat.2016.06.022
6. Saiyathibrahim, A., Subramaniyan, R., Dhanapl, P. (2016), *Centrefugally cast functionally graded materials – A review*. Int. Conf. on Systems, Science, Control, Comm., Eng. and Techn. (ICSSCCET 2016), 02: 68-73.
7. Hutchinson, W., Suo, Z. (1991), *Mixed mode cracking in layered materials,* Advances in Applied Mechanic, 29: 63-191. doi: 10.1016/S0065-2156(08)70164-9
8. Rizov, V.I. (2017), *Delamination fracture in a functionally graded multilayered beam with material nonlinearity*, Archive of Applied Mechanics, 87(6):1037-1048. doi: 10.1007/s00419-017-1229-x
9. Rizov, V.I. (2017), *Non-linear elastic delamination of multilayered functionally graded beam*, Multidisc. Model. Mater. Struc. 13(3): 434-447. doi: 10.1108/MMMS-10-2016-0054
10. Rizov, V.I. (2017), *Delamination of multilayered functionally graded beams with material nonlinearity*, Int. J Struc. Stability Dynam. 18(04), doi.org/10.1142/S0219455418500517
11. Rizov, V.I. (2018), *Analysis of delamination in two-dimensional functionally graded multilayered beam with non-linear behaviour of material*, Eng. Trans., 66(1): 61-78.
12. Rizov, V.I. (2018), *Delamination in multi-layered functionally graded beams – an analytical study by using the Ramberg-Osgood equation*, Struc. Integ. and Life, 18(1), 70-76.
13. Broek, D., Elementary Engineering Fracture Mechanics, Springer, 1986.